Title
Overview of Remote Sensing and GIS Uses in Watershed and TMDL Analyses

Journal
Journal of Hydrologic Engineering, 24(4)

ISSN
1084-0699

Authors
Quinn, Nigel WT
Kumar, Saurav
Imen, Sanaz

Publication Date
2019-04-01

DOI
10.1061/(asce)he.1943-5584.0001742

Peer reviewed

Overview of Remote Sensing and GIS Uses in Watershed and TMDL Analyses

Nigel W. T. Quinn, Ph.D., P.E., D.WRE, F.ASCE

Research Group Leader, Hydro-Ecological Engineering Advanced Decision Support, Berkeley National Laboratory, 1 Cyclotron Rd. Bldg., 64-209, Berkeley, CA 94720 (corresponding author). Email: nwquinn@lbl.gov

Saurav Kumar, Ph.D., A.M.ASCE

Research Assistant Professor, Dept. of Civil Engineering, Univ. of Texas at El Paso, El Paso, TX 79968.

Sanaz Imen, Ph.D.

Civil Engineer, Stantec Engineering Services Company, One Biscayne Tower Suite 1670, 2 South Biscayne Blvd., Miami, FL 33134.

Introduction

Advances in remote sensing approaches have provided the capability to acquire water quality information at spatial and temporal resolutions beyond the capability of periodic and in situ measurements at measuring points. By integrating remote sensing data with geographic information systems, more-comprehensive analysis of water quality has become possible. Optical and thermal sensors, when deployed on boats, aircraft, or satellites, can provide both the spatial and temporal information needed to understand changes in water quality characteristics which are often the same characteristics essential for developing better management practices to improve water quality.

Spatially distributed, parametric Total Maximum Daily Load (TMDL) models require topographic, soil, and land-use information as input data (Doherty and Simmons 2013). GIS and remote sensing have been adopted as useful tools for processing raw data to provide model input and for synthesizing spatial data (Kang 2002; Kang and Park 2003) as part of the modeling process. There are many examples of the use of a GIS as both preprocessor and postprocessor to TMDL models—both the Better Assessment Science Integrating Point and Nonpoint Sources (BASINS version 4.1) and Watershed Analysis Risk Management Framework (WARMF) models specifically include GIS (ASCE 2017). If included as part of a model framework, a preprocessor typically provides formatted input data from individual or combined GIS data layers, whereas postprocessors can be used to aid visualization of model output and to graphically display simulation results (Kang et al. 2006). Where this visualization is a map, the GIS is especially useful.

Spatial modeling of data, which includes preparing maps with water quality and other key geomorphological information, may be done using most GIS and helps decision makers to develop a comprehensive view of the target area for TMDL development. Initial spatial modeling may also help in selecting and organizing data in a required format for input to water quality (watershed and receiving water) models used in TMDL development. Several examples of this preprocessing approach are available in the literature in which initial preprocessing is done using GIS (Shafique et al. 2003; Ramirez et al. 2005; Viers et al. 2005). Furthermore, GIS also have a critical role to play in the postprocessing of modeled results and planning remediation or abatement strategies, such as citing structural best management practices and targeting nonstructural best management practices to high-impact areas.

Most modern water quality models used for TMDL modeling require one or more spatially referenced data sets as input (ASCE 2017). These data sets are often obtained from multiple sources and may have different projections and spatial scales. This diversity of information formats makes GISs such as ArcGIS, QGIS, and GRASS that are designed for handling spatially referenced data obvious choices for data management and processing. Specialized software designed for digital elevation processing, such as TOPAZ, TauDEM version 5, and BASINS, along with libraries and modules available within most GIS, such as spatial analyst in ArcGIS, catchment area in QGIS, and watershed in Geographic Resources Analysis Support System (GRASS), may be of assistance in converting digital elevations to the topographic information required to develop the hydrology that creates the fluxes important for most water quality models. Suites of proprietary software such as Aquaveo WMS 10.1 have been coupled with several widely used water resources models such as Storm Water Management Model (SWMM version 5.1.013), Gridded Surface Subsurface Hydrologic Analysis (GSSHA), Hydrological Simulation Program—Fortran (HSPF version 11.0), and CE-QUAL-W2 to make the task of executing models easier by preprocessing data and visualizing output from multiple water quality models (ASCE 2017). Proprietary extensions are also available to integrate ArcGIS with several other water quality models, such as InfoSWMM (2017) for SWMM and ArcSWAT for Soil & Water Assessment Tool (SWAT).

Remote Sensing Sensors and Platforms

Certain water quality parameters of interest have well-defined spectral properties which yield unique spectral curves. This characteristic facilitates separating and distinguishing these water quality parameters in a water body. Sensors mounted on satellites and other platforms can measure the natural reflectance of the target (passive sensing) or measure radiation emitted by the target being investigated (active sensing). Three spectral bands, visible (VIS), infrared (IR), and microwave (MW), are the most measured spectral bands for remote sensing in water bodies (Richards 1986). A guide to the evolution of satellite remote sensing sensors and platforms is shown in Fig. 1 in basic chronological order. The first artificial Earth satellite was Sputnik-1, launched in 1957 by the Soviet Union to broadcast radio pulses. Three years later, the first successful low-Earth-orbit weather satellite TIROS-1 was launched and placed into orbit. Nimbus 1, 2, and 3 were the second-generation US satellites, launched in the 1960s to perform advanced meteorological research. In 1972, the first satellite operated by the US Landsat

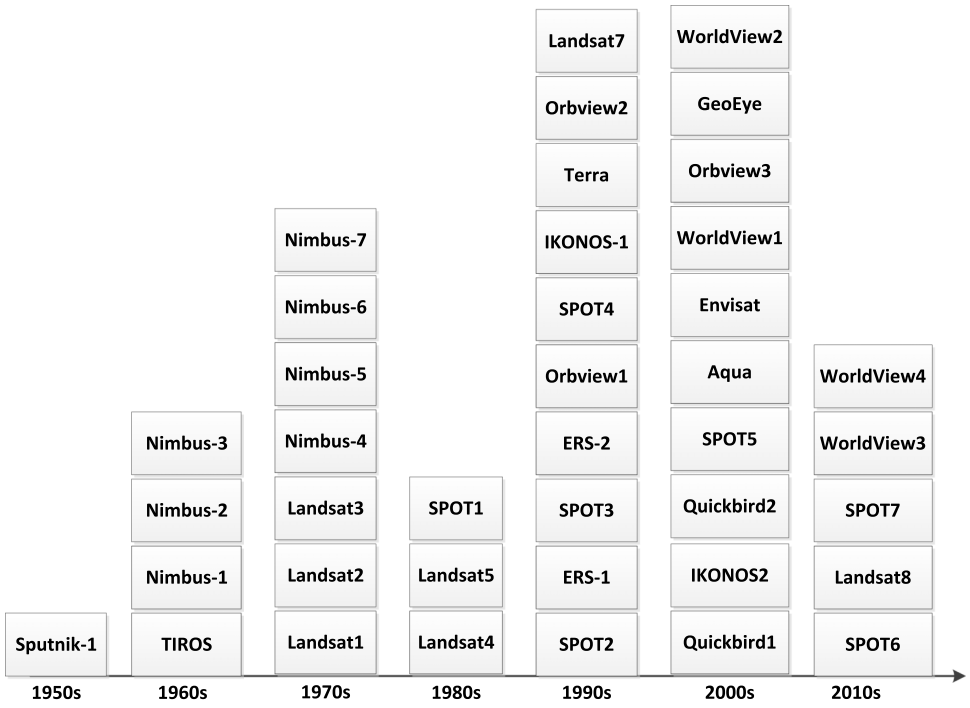

Fig. 1. Chronological evolution of some important satellites since the 1950s.

program was launched to obtain information on agriculture, environmental pollution, oceanography, and metrological phenomena. Landsats 2 and 3 were launched in 1975 and 1978, respectively. Landsat 3 had an improved 38-m ground resolution and used two RCA cameras which both imaged in one broad spectral band rather than three separate bands. In the 1970s, the second generation of Nimbus satellites (Nimbus 4–7) was launched. The fourth satellite of the Landsat program was launched in 1982 to provide a global archive of satellite imagery. Landsat 4 was the first satellite in the Landsat program that had a Thematic Mapper (TM) sensor which enabled much higher resolution than the previously deployed multispectral scanner. In addition, the orbiting time of Landsat 4 was decreased from 18 days to 16 days. The other satellite of the Landsat program (Landsat 5) was launched in 1984. It was a low-Earth-orbit satellite which had similar spectral and spatial resolution and sensors as Landsat 4. In Landsat 6, the TM sensor was replaced with an Enhanced Thematic Mapper (ETM) sensor to add a 15-m resolution panchromatic band. However, this satellite failed to reach the intended earth orbit. The seventh satellite of the Landsat program was launched in 1997. The main sensor on board Landsat 7 is the Enhanced Thematic Mapper Plus (ETM+). It has a revisit time of 16 days and differs from the previous satellites in the Jenson (2013) Landsat program by virtue of its enhanced physical memory storage capability of 378 gigabits (about 100 images) of Landsat 7. The last satellite of the Landsat program was launched in 2013 to collect medium-resolution (30-m) multispectral image data to provide essential information on land cover and land-use change over time—high-priority data for climate change assessments.

In 1986, the first Satellite Pour l'Observation de la Terre (SPOT) program satellite was launched by the French space agency to improve the knowledge of the Earth by detecting and monitoring climate and land-use phenomena related to human activities. SPOT 2, 3, and 4 were launched in 1990, 1993, and 1998, respectively. All these SPOT satellites had the same imaging instruments, including two identical high-resolution visible (HRV) imaging instruments that offered panchromatic band with 10-m resolution and three multispectral bands with 20-m resolution. SPOT 1, 2, and 3 had revisit times of 1–4 days. However, SPOT 4 had a revisit time of 5 days. To improve the quality of images (2.5–5 m) and ensure continuity of services, the SPOT program launched three additional satellites in 2002, 2012, and 2014.

In the 1990s, the European Space Agency (ESA) developed a specialized instrument called synthetic aperture radar (SAR) to produce high-quality images regardless of weather conditions, cloud coverage, and daylight or night conditions. SAR was deployed on the ERS-1 and ERS2-2 satellites, giving them the ability to capture high-resolution imagery of the oceans, coastal zones, polar ice, and land regions. The first satellite of the OrbView program was launched in 1995 by NASA. OrbView-1 has two sensors, an optical transient detector and an atmospheric monitoring instrument. This satellite provides information of severe weather patterns and cloud-to-cloud lightning data. The second satellite of the OrbView program, OrbView-2 was launched in 1997 to provide information used for research in biogeochemical processes, climate change, and oceanography. It operated the SeaWiFS sensor for NASA and had a daily revisit time with moderate resolution. The last satellite of OrbView program was launched in 2007 and is able to provide 1-m panchromatic imagery and 4-m resolution in the multispectral mode with a 3-day revisit time.

DigitalGlobe launched two IKONOS satellites in 1999 and 2000. IKONOS were high-resolution satellites with a capability of capturing 3.2-m multispectral and 0.82-m panchromatic images at nadir. The popularity and relatively low cost of this imagery helped improve both urban and urban mapping of natural resources, agriculture and forestry resources, and mining areas, and aided vegetation change detection. In the 2000s, DigitalGlobe launched another high-resolution earth observation satellite, QuickBird, which collected panchromatic imagery at a 61-cm resolution and multispectral imagery at a 2.44–1.63-m resolution. GeoEye-1 is another satellite launched by DigitalGlobe, which provides a resolution of 0.46 m. Additional satellites that DigitalGlobe launched in the 2000s and 2010s were named WorldView. The WorldView-1 satellite has

an average revisit time of 1.7 days with a panchromatic imaging system with 0.46-m resolution. The WorldView-2 satellite is able to collect a large area of multispectral imagery in a single pass with a revisit time of 1.1 days. The WorldView-3 and WorldView-4 satellites provide similar panchromatic imagery with 0.31-m resolution and eight-band multispectral imagery with 1.24-m resolution.

In 1999, the Terra satellite was launched, and it began collecting imagery in February 2000. The Terra satellite has 5 remote sensors on board: Advanced Spaceborne Thermal Emission and Reflection Radiometer (ASTER), Clouds and the Earth's Radiant Energy System (CERES), Multi-angle Imaging SpectroRadiometer (MISR), Moderate-resolution Imaging Spectroradiometer (MODIS), and Measurements of Pollution in the Troposphere (MOPITT). The main goal of launching this satellite was to provide information on the spread of pollution around the globe. The Aqua Earth-observing satellite was launched in 2002 to transmit high-quality data and collect information about the Earth's water cycle. In addition, it collects information about the vegetation cover, phytoplankton, dissolved organic matter, and water temperature. This satellite collects this information using six instruments on board: Atmospheric Infrared Sounder (AIRS), Advanced Microwave Sounding Unit (AMSU), CERES, MODIS, Advanced Microwave Scanning Radiometer-EOS (AMSR-E), and Humidity Sounder for Brazil (HSB). Another Earth-observation satellite is Envisat, launched in 2002 to improve environmental studies. It has nine instruments on board: Medium Resolution Imaging Spectrometer (MERIS), Advanced Along Track Scanning Radiometer (AATSR), Scanning Imaging Absorption Spectrometer for Atmospheric Chartography (SCIAMACHY), Radar Altimeter 2 (RA-2), Microwave Radiometer (MWR), Doppler Orbitography and Radiopositioning Integrated by Satellite (DORIS), Michelson Interferometer for Passive Atmospheric Sounding (MIPAS), Global Ozone Monitoring by Occultation of Stars (GOMOS), and Advanced Synthetic Aperture Radar (ASAR).

As the cost of imagery and processing software has fallen over the last decade and access to simple graphical user interfaces has increased for the more popular image processing tools such as ERDAS, ENVI, and ARCGIS Image Analyst, these data resources are increasingly being used in basin-scale simulation modeling studies and TMDLs (ASCE 2017). Whereas in the past, remote sensing analysis was conducted independently from model development—incorporated into model input files through the use of GIS as an intermediary product—several model preprocessors now allow direct use of remote-sensing data products.

Image Processing Techniques

Satellite imagery is captured at a great distance from the Earth's surface, and electromagnetic energy passes through a substantial atmospheric path to reach to sensors. Atmospheric particles may absorb or scatter the radiation. In addition, satellites follow an orbit relative to the Earth while the satellite imagery is being processed. The relative movement of the Earth may cause a displacement in the path of the satellite that needs to be recognized in the image analysis. Processing of satellite imagery to correct errors and minimize distortion helps to rectify images to correctly represent conditions on the Earth' surface and provide the highest possible data quality prior to analysis and interpretation (Chang et al. 2015). The techniques of processing satellite imagery can be divided into two major operations, namely radiometric correction and geometric correction. Internal radiometric errors are caused by sensor malfunction or poor calibration of sensors. External radiometric errors are typically caused by atmospheric absorption. Radiometric correction is made using *calibration* data between measured irradiance and the sensor output, and can be performed using a variety of methods, including image-based methods, radiative transfer models, and the empirical line method (Chang et al. 2015). Radiometric calibration and correction are particularly important when comparing data sets over a multiple periods to improve the interpretability and quality of the remotely sensed data.

Scan skew, earth rotation, platform velocity, mirror scan velocity, panoramic distortion, and perspective distortion lead to systematic geometric errors. The variation in the distance between the Earth and the platform may cause nonsystematic geometric errors. Geometric correction can be performed using available data about platform ephemeris, points on the Earth's surface with available map coordinates, image-to-map rectification, and image-to-image rectification.

Use of remotely sensed imagery in TMDL modeling will be significantly enhanced by automation of the data quality assurance procedures relevant to remotely sensed data. The urgency for this development comes from the explosion of new remote-sensing platforms such as drones which have driven down the cost of imagery acquisition and created a need for fast and uncomplicated data quality screening and correction automation, especially for scientific research deployments. Other remote-sensing technologies are seeing similar migration to the public domain.

Overview of Relevant Remote-Sensing Technologies

LIDAR

Light detection and ranging (LIDAR) is an active remote sensing technology which records laser pulses to detect an object and determine the distance between the instrument and the object (range). Based on the interaction of the radiation with an object, physical properties of an object are detected (Diaz et al. 2013). LIDAR has several applications, such as agriculture, forest planning and management, forest fire management, environmental assessment, flood modeling, watershed and stream delineation, ecological and land classification, river surveying, pollution modeling, management of coastlines, monitoring glacier volume changes, and meteorology. LIDAR data analysis and interpretation has been incorporated into several GIS software platforms, such as ArcGIS.

Multispectral Remote-Sensing Imagery

Multispectral imagery is produced by sensors that capture the backscattered energy from an object in multiple bands (3–10 bands) of the electromagnetic spectrum (Al-Mulla 2010). Types of sensors used in multispectral remote sensing include line detector, whiskbroom, and pushbroom. The line detector sensor detects only one object at a time. The whiskbroom scanner scans the Earth in a series of lines that are perpendicular to the direction of motion of the sensor platform. A rotating mirror is applied to scan from one side to the other. A bank of internal detectors measures the energy for each spectral band, converts the analog signal to digital data, and stores the data record for further processing. The pushbroom scanner also scans the Earth in a series of lines using track scanning. Pushbroom motion and its array of detectors leads to energy capture from each ground resolution cell for a longer period. Hence the pushbroom scanner has a higher spatial and spectral resolution than the whiskbroom scanner. Multispectral imagery from platforms such as Landsat is now offered at no cost to the public by the Department of the Interior through the offices of the USGS. This has led to an explosion of applications including the popular Google Earth Engine platform, which provides real-time processing of Landsat imagery around the world. Early applications of the technology included

analysis of deforestation and reforestation rates globally and estimation of daily agricultural crop evapotranspiration using a technique that detects hot and cold pixels in the Landsat scene and relates these to minimum and maximum evapotranspiration rates using measured weather station data and derived estimates of reference evapotranspiration. The latter application could provide significant technical and economic benefits to irrigated agriculture around the world once the procedures for cloud-cover masking and recognition of image artifacts is perfected and the software application is made more robust.

Hyperspectral Sensing for TMDL Modeling

Hyperspectral imaging, or imaging spectroscopy, like other passive remote sensing methods, is used to measure the spectral signatures of features using the Sun's energy reflected or remitted from the feature. The criteria that discriminate various remote-sensing methods are the spectral bandwidths and the number of bands. The spectral bandwidth in hyperspectral sensing is lower than that for multispectral and broadband imaging; at the same time, the number of bands in a hyperspectral image is far greater. This higher spectral resolution allows better identification, characterization, quantification, and subpixel detection (detection in sizes less than the spatial resolution) with hyperspectral imaging. The properties of hyperspectral imaging may be particularly useful in acquiring data for TMDL modeling and assessing the outcomes of TMDL implementation for large and small watersheds. The key challenges in acquiring and utilizing hyperspectral sensing data are the problems with the cost of acquisition and the difficulty in processing (Ramirez et al. 2005). The sensors used to acquire these data, particularly through airborne platforms, are expensive and need specialized handling. Several spaceborne platforms have also been equipped with hyperspectral sensors which may alleviate the problems of data acquisition; however, these platforms often have limited spatial resolutions. There are other sources of hyperspectral data, such as the NASA Airborne Visible Infrared Imaging Spectrometer (AVIRIS). Data from most AVIRIS flights are available through a designated web portal (AVIRIS 2018). Hyperspectral data contains both spatial and spectral information. The data collected from a hyperspectral sensor may be thought of as a collection of overlaid spatial raster layers, with each layer representing reflectance at a wavelength, resulting in a data cube. With hundreds of spectral bands, large amounts of data are usually collected, depending on the spatial resolution and area covered, and then processed to remove atmospheric effects (Gao et al. 2009; Zarco-Tejada and González-Dugo 2012). Methods are also adopted for removing redundant and noisy data (Chang 2013).

Overview of Relevant GIS Technologies

The first-generation GIS, developed in the 1960s and 1970s, were generalized CAD-based mapping systems that stored geographic information in file formats that represented points, lines, and areas, and had a limited ability to store attribute data. The field has evolved dramatically in the last 40 years, with the development of relational databases and the portioning of spatial and attribute data, allowing the coverage data model to become the kernel of the GIS. More-recent innovations in object-oriented software design have led to the introduction of the geodatabase model, first released by ESRI with version 8 of ArcGIS software. This GIS architecture provides flexibility in the definition and behavior of data objects, allowing relationships to be defined in terms of their topological and spatial features in new ways (Zeiler 1999). This architecture creates a unified data model which allows easier linkage to models used for TMDL analysis.

GIS Data Processing

Once point, line, or area feature data have been imported to a GIS and georeferenced, further processing and manipulation of the data can yield useful output for simulation modeling. For example, Fig. 2 shows a map of the subsurface tile drainage mains and laterals in a water district in the San Joaquin Basin of California. Using the polygon interest and line data processing features of ArcGIS version 10.6, the linear lengths of lateral and mainline drains were summed within each 1-mi^2 model cell (shown in outline superimposed on the drainage map). The drainage yield and conductance terms in the groundwater simulation model are directly related to the total drain length and a calibration factor which produces a drainage volume per unit of head difference between the drain elevation and the water table and the linear length of drain. Previous iterations of the model developed a function related only to the hydraulic head difference between the drain depth and water table; the new algorithm allows greater disaggregation of drainage estimates.

A second example of GIS data processing is illustrated in Fig. 3, which shows the use of a software robot which traverses the nodal map of a numerical groundwater model of the San Joaquin Basin of California and associated digital DEM data and helps assign model groundwater nodes to corresponding model river nodes. The river nodes represent the San Joaquin River, which drains the Basin and is the receiving water for a salinity TMDL. Ephemeral streams that truncate prior to meeting the San Joaquin River had their discharge assigned to groundwater nodes, which in turn were assigned to multiple San Joaquin River nodes along corridors that connect the interior groundwater nodes with the River. The Euclidean point–processing algorithm used in the analysis provided a logical and repeatable methodology for linking the groundwater and surface water component models that together determined the flow and water quality interaction between surface and groundwater systems that were critical for completion of a credible water quality TMDL.

Overlay Analysis

Not only is GIS able to store digital data in multiple layers, it also is able to generate a new data layer using the attributes of all existing layers taking part in overlay analysis (Jensen and Jensen 2017). This process can be performed in either feature or raster systems. Feature overlay includes overlaying points, lines, or polygons. Output of a feature system depends on the type of overlaid features. For instance, overlaying polygons leads to the creation of new areas. However, overlaying a line with polygons produces lines that have features of both the original line and polygons. The raster system, which is known as grid overlay, is only able to combine attributes of exactly aligned grids. Otherwise, the misaligned grids need to be resampled. One of the most important steps prior to overlay analysis is to reference all layers to the same coordinate system, the same datum, and the same map projection.

ESRI (2017) defined eight general steps of overlay analysis. The first step of overlay analysis is defining the problem. The overall objective and the concept of the problem must be identified. It is also necessary to understand when the problem is solved. The next step is breaking the problem into submodels to be able to focus on different components of a problem (cost, risk, and so on). The third step is determining the attributes or layers that contribute to the goals of each submodel. Different layers have different ranges of values. It is not possible to combine different number systems. For this purpose, common scales need to be defined for all layers;

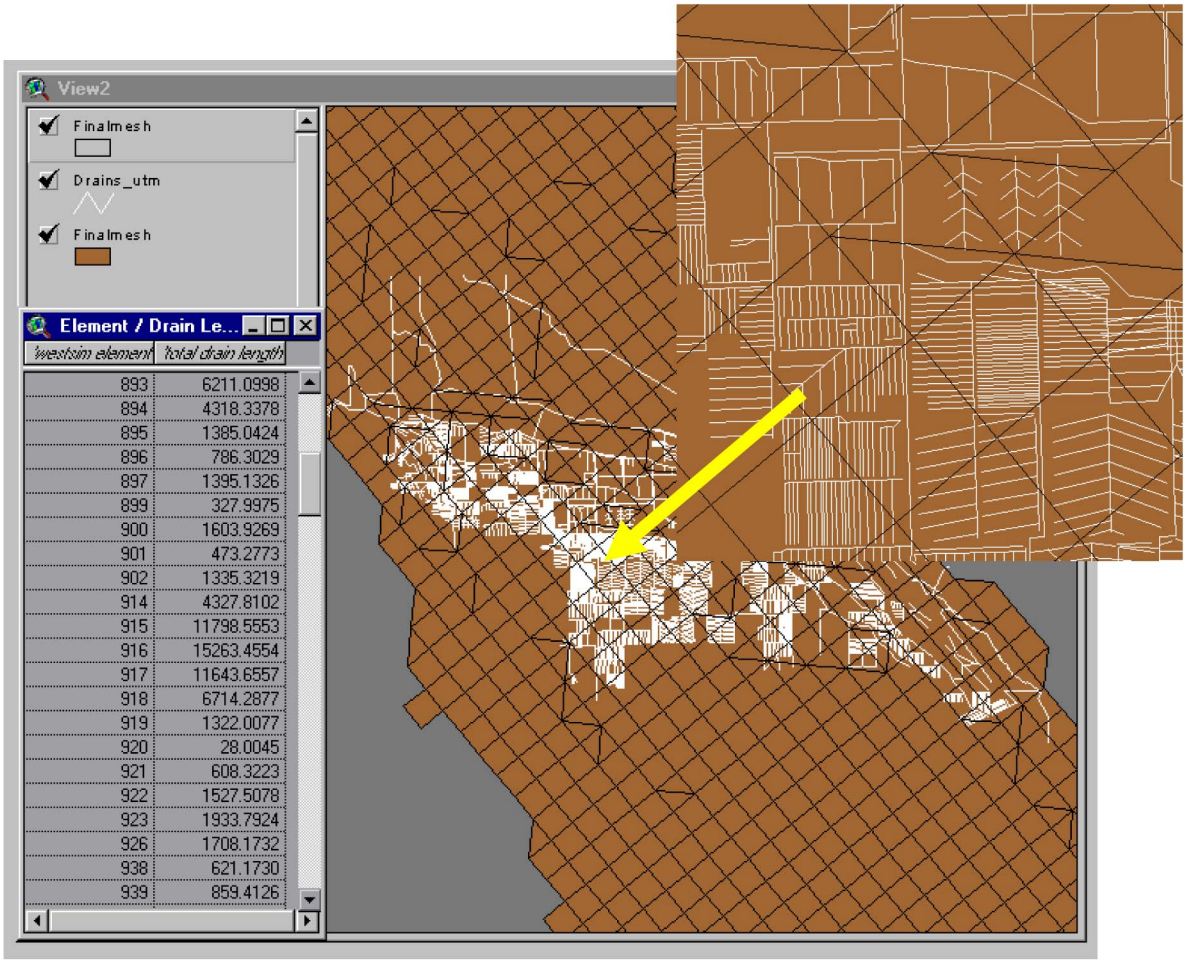

Fig. 2. Computation of subsurface drainage tile length using a GIS and line features from a water district drainage map. The model cell drainage conductance is directly correlated with tile drain length.

for instance, scales of 1–10, in which the higher value is more favorable. Some factors may play more important roles than others. Therefore, prior to combining different factors (Step 6), the factors can be weighted based on their importance. In order to select the best location (Step 7), ArcGIS provides a tool that allow the user to identify the best combinations of desired regions. The final step is analyzing the results. It may be beneficial to determine the second and third most favorable sites in addition to identifying the best location.

GIS Modeling

Bolstad (2016) considered three types of GIS models: cartographic models, spatiotemporal models, and network models. Cartographic models are usually temporally static, involve combined spatial data sets, and rely on specific operations and functions for problem solving. These models apply weights and ranking to important features or criteria, and are commonly used for applications such as suitability ranking. Simple linear models such as the Universal Soil Loss Equation, primarily used for estimation of runoff and soil erosion from agricultural land, is a good example of this type of GIS modeling application. Most of the model parameter inputs of soil erodibility, rainfall erosivity, cropping practices, and management can be mapped spatially as model inputs.

Spatiotemporal models simulate time-driven processes and their dynamics in both space and time. These are typical of the models used in most TMDL analyses which are iterative, require sets of initial conditions, and produce time series predictions of key state variables as output. These models can be descriptive or prescriptive, stochastic or deterministic, and either inductive or deductive, but all represent meaningful features in the landscape and simulate events and processes in geographic space. Early versions of these models provided a means of creating input data sets from GIS maps; more temporary models are fully integrated (ASCE 2017). Network models are mostly concerned with the simulation of resources—their flow, accumulation, or depletion—within well-defined networks. This type of model is not commonly used in TMDL development.

Integrated GIS Modeling

Integrated modeling systems imply an integration of data and knowledge from across relevant science domains within the computational form of a conceptual model. Laniak et al. (2013) considered integrated environmental modeling as a landscape containing four interdependent elements: applications, science, technology, and community. Contemporary environmental modeling systems include science models, user interfaces, data analysis and visualization tools (including GIS), and calibration and optimization tools (Doherty and Simmons 2013; Doherty and Hunt 2010). Interoperability is needed between these tools to simplify and automate data transfer across applications so that the tools appropriately address their combined function (Laniak et al. 2013).

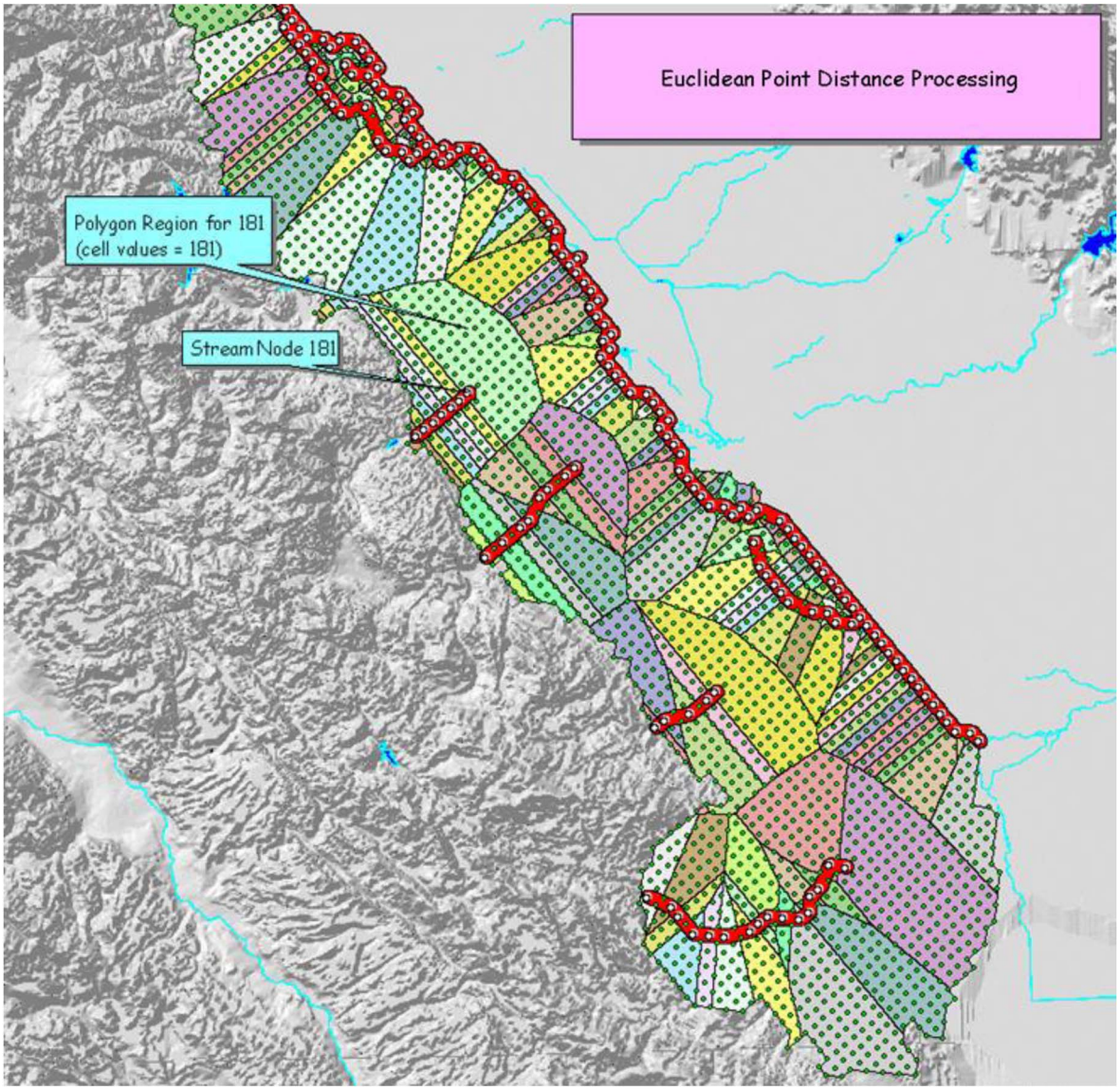

Fig. 3. Use of GIS to determine likely flow paths from groundwater nodes and the ephemeral streams emanating from the Coast Range mountains to the San Joaquin River. A robot used the digital DEM data to link each groundwater and stream node with a single stream node on the San Joaquin River.

Integrated modeling frameworks can help to maintain some level of local control over the user experience, in particular the design and implementation of the graphical user interface (GUI), which has been found to be an important attribute for buy-in and effective function within user communities. Less-structured integration of models can be facilitated with software products such as OpenMI, which provides a protocol for exchanging data among linked models at run time (Moore and Tindall 2005). GIS can provide a service during model integration by forcing models to recognize a common geographic frame of reference and explicit linkage between model nodes and areas on maps. Spending time on this georeferencing of model hydrology early can avoid mass balance errors and potential model instability when models are linked or coupled later.

Remote Sensing in Hydrologic and Water Quality Modeling

Total maximum daily load calculations are used by states and the USEPA to limit both point-source and non-point-source pollution by establishing water quality objectives for receiving waters and limiting watershed pollutant loading into these receiving waters in a manner consistent with meeting these water quality objectives. TMDLs have been developed for a variety of pollutants that impair or threaten the intended beneficial uses of a water body. Key pollutants for which TMDLs have been developed include sediments, pathogens, nutrients, metals, dissolved oxygen, temperature, pH, mercury, pesticides, and organics (USEPA 2011). Remote-sensing applications are limited to those substances or conditions that can influence and change the optical (reflected) or thermal characteristics of the water surface, such as suspended sediments and temperature. Other pollutants can be measured indirectly utilizing techniques through surrogate indicators. For example, chlorophyll *a* is a characteristic of algal biomass that has a unique reflectance and can be a useful indicator of elevated nutrient levels.

Remote sensing and GIS can also be used in formulating management plans that can result in improvements to the quality of impaired waters. Effective TMDL implementation plans can be developed by enhancing land-use planning using remote sensing

Table 1. Examples or case studies combining GIS and remote sensing for watershed modeling

Reference	Water resources model	GIS and remote sensing information	GIS software	Purposes	Region	Watershedarea (km^2)	Linkage type
Amatya et al. (2008, 2011)	ArcView SWAT	Elevation: South Carolina Department of Natural Resources, derived from USGS quadrangle map Soil: SSURGO database Land use: NAIP Imagery	ArcGIS	TMDL and BMP development	Chapel Branch Creek, Santee, South Carolina	16	Combined
Bhuyan et al. (2002)	AGNPS	Elevation: USGS DEM 30m Soil: Soil database from Kansas Data Access Support Center Land use: Derived from Landsat Thematic Mapper	ArcGIS	Land-use decisions, BMP development	Cheney Reservoir watershed in south central Kansas	2,404	Linked
Kang et al. (2006)	ArcView SWAT	Land use: Derived from Landsat Thematic Mapper	ArcGIS	TMDL and BMP development, visualization	Korea	30	Combined
Di Luzio et al. (2004)	ArcView SWAT	Elevation: USGS DEM 30m and DEM 90m Soil: NRCS county soil survey map, STATSGO soil map Land use: Derived from Landsat Thematic Mapper	ArcGIS	TMDL and BMP development	Goodwin Creek watershed, Yazoo River, Mississippi	21	Combined
Ning et al. (2002)	GWLF	Land use: Derived from SPOT satellite data	ArcGIS, ERDAS IMAGINE	TMDL, loading estimation	Kao-Ping River Basin, Taiwan	3,256	Linked
Strager et al. (2010)	Based on export coefficient, loading capacity, average loads, no GW flow, and all pollutants are conservative	Elevation: USGS DEM	ArcGIS 9.x	Mining DSS, site screening model, multicriteria decision making	West Virginia; may be applied to other places	variable	Integrated
Yuan et al. (2006)	AnnAGNPS		ArcGIS	Identifying disturbed land-use types	Bayou Lafourche watershed, Louisiana	1,461	Combined

and GIS to reduce pollutant movements to the water body (Zaidi 2012).

The thermal band of satellite data can be used to estimate the surface temperature of water bodies. Other variables that cannot be quantified through satellite data, such as bacteria and nutrient loads, sometimes can be assessed using surrogate indicators, which can be field-validated. Multitemporal satellite data are required for this purpose. For land-use/land-cover classification, medium-spatial-resolution Landsat satellite data are a publicly available product that is commonly used. Multispectral data from Earth-observing satellite SPOT 5 and Landsat 7 data may be utilized for establishing spatial relationship between satellite data and field-measured water quality parameters. True-color orthophotography at much higher resolutions is also useful for detecting impervious cover and forests at much higher resolutions, which is useful for small watersheds.

GISs in Hydrologic, Water Quality, and TMDL Modeling

In their assessment of available models, Kang et al. (2006) addressed the impact of best management practices on the studied water bodies, providing guidance for more-effective implementation of TMDL programs. The total maximum daily load system (TOLOS) is another example of a GIS ArcView SWAT (AVSWAT) application, which has proved useful for developing and evaluating TMDLs in small watersheds containing rice paddies in the Republic of Korea.

Several interfaces of GIS with water resources models have been developed, some of which are listed in Table 1. Models including HSPF, SWAT, and SWMM, have been coupled with GIS for preprocessing and postprocessing using extensions to standard GIS. For example, HSPF has been coupled with WMS and BASINS. An extension for ArcGIS is available for preprocessing HSPF data. Similar ArcGIS extensions are also available for SWAT, SWMM, Agricultural Policy/Environmental eXtender (APEX), and AnnAGNPS. Other models such as WARMF have built-in GUIs with geoprocessing capacity for preprocessing and postprocessing.

Using the terminology defined by Martin et al. (2005), GIS–water resources model interfaces may be linked in three groups: linked, combined, and integrated. A water resources model linked with a GIS requires manual data exchange between the model and the GIS.

- Linked-type interfaces are the simplest to develop and are very flexible, independent of either the modeling or GIS software. However, often such approaches are not standardized and do not use the full power of the GIS and the spatial relations in the data sets.
- Combined water resources models and GIS software have automated data exchange; although more robust, this exchange can be more difficult to program and more inflexible in terms of the combined software compared with linked models.
- Integrated water resources models and GIS software usually have the water resources model programmed in the GIS or the GIS built into the water resources model. Data exchanges in such scenarios are transparent to the end-user, and the framework can use the power of the GIS; however, such systems tend to simplify the water resources models.

Several models with combined-type links are available, such as AVSWAT (Di Luzio et al. 2004) and may not need any additional programming to connect the model with the GIS. However, to apply such models, depending on the characteristics of the local area, special GIS processing may be needed. For example, Amatya et al. (2008), using AVSWAT, reported that hand-digitizing stream lines from aerial photographs improved the flow routing computed by the combined model.

Conclusions

Most water resources models currently used were developed before GIS matured and were standardized. Consequently, several water resources models are not well integrated with GIS for spatial-data management, visualization, or modeling to support decision making for TMDL development. Martin et al. (2005) in their review of the GIS interfaces with water resources models pointed out that neither of the technologies were developed to interact with each other. This has led to present-era systems that interface GIS with robust peer-reviewed modeling tools in the three ways described previously. Nevertheless, significant advancements have been made in the last decade which enable gainful use of GIS and remote sensing for water resources modeling, especially for TMDL development. For example, several water resources models have extensions to link this software to ArcGIS, which simplifies the task of processing information and the resulting analysis. Integration with open-source and free GIS, however, has been lacking. Similarly, web-based GIS that have the capacity to make water resources models more widely available to the stakeholders had not been widely adopted by the modeling community as of 2016. These developments have implications for the next generation of TMDL modeling endeavors.

References

Al-Mulla, Y. A. 2010. "Salinity mapping in Oman using remote sensing tools: Status and trends." *A monograph on management of salt-affected soils and water for sustainable agriculture*, 17–24. Oman: Sultan Qaboos Univ.

Amatya, D. M., J. Manoj, A. E. Edwards, T. M. Williams, and D. R. Hitchcock. 2011. "SWAT-based streamflow and embayment modeling of karst affected Chapel Branch watershed, SC." *Trans. Am. Soc. Agric. Biol. Eng.* 54 (4): 1311–1323.

Amatya, D. M., T. M. Williams, A. E. Edwards, N. S. Levine, and D. R. Hitchcock. 2008. "Application of SWAT hydrologic model for TMDL development on Chapel Branch Creek watershed, SC." In *Proc., South Carolina Water Resources Conf.* Charleston, SC: Public Service and Agriculture (PSA)'s South Carolina Water Resource Center.

ASCE. 2017. *Total maximum daily load analysis and modeling: Assessment of the practice*. Reston, VA: ASCE.

AVIRIS (Airborne Visible Infrared Imaging Spectrometer). 2018. "Airborne visible/infrared imaging spectrometer." Accessed July 15, 2017. https://aviris.jpl.nasa.gov/.

Bhuyan, S. J., L. J. Marzen, J. K. Koelliker, J. A. Harrington Jr., and P. L. Barnes. 2002. "Assessment of runoff and sediment yield using remote sensing, GIS and AGNPS." *J. Soil Water Conserv.* 57 (6): 351–364.

Bolstad, P. 2016. *GIS fundamentals: A first text on geographic information systems*. Annecy-le-Vieux, France: Eider Press.

Chang, C. 2013. *Hyperspectral data processing: Algorithm design and analysis*, 1164. New York: Wiley.

Chang, N. B., S. Imen, and B. Vannah. 2015. "Remote sensing for monitoring surface water quality status and ecosystem state in relation to nutrient cycle: A 40-year perspective." *Crit. Rev. Environ. Sci. Technol.* 45 (2): 101–166. https://doi.org/10.1080/10643389.2013.829981.

Diaz, J. C. F., W. E. Carter, R. L. Shrestha, and C. L. Glennie. 2013. "Lidar remote sensing." In *Handbook of satellite applications*, 757–808. New York: Springer.

Di Luzio, M., R. Srinivasan, and J. G. Arnold. 2004. "A GIS-coupled hydrological model system for the watershed assessment of agricultural nonpoint and point sources of pollution." *Trans. GIS* 8 (1): 113–136. https://doi.org/10.1111/j.1467-9671.2004.00170.x.

Doherty, J. E., and R. J. Hunt. 2010. *Approaches to highly parameterized inversion—A guide to using PEST for groundwater-model calibration*. US Geological Survey Scientific Investigations Rep. No. 2010-5169. Reston, VA: USGS.

Doherty, J. E., and C. T. Simmons. 2013. "Groundwater modelling in decision support: Reflections on a unified conceptual framework." *Hydrogeol. J.* 21 (7): 1531–1537. https://doi.org.10.1007/s10040-013-1027-7.

ESRI (Environmental Systems Research Institute). 2017." Understanding overlay analysis." Accessed September 22, 2014. https://desktop.arcgis.com/en/arcmap/latest/tools/spatial-analyst-toolbox/understanding-overlay-analysis.htm.

Gao, B., M. Montes, C. Davis, and A. Goetz. 2009. "Atmospheric correction algorithms for hyperspectral remote sensing data of land and ocean." *Remote Sens. Environ.* 113 (1): S17–S24. https://doi.org/10.1016/j.rse.2007.12.015.

InfoSWMM. 2017. "Sophisticated geospatial urban drainage modeling." Accessed September 22, 2014. https://www.innovyze.com/products/infoswmm/.

Jensen, J. R., and R. R. Jensen. 2017. *Introductory geographic information systems: Pearson series in geographic information science*. 1st ed. London: Pearson Higher Education.

Jenson, J. R. 2013. *Introductory geographic information systems*. London: Pearson Education.

Kang, M. S. 2002. "Development of total maximum daily loads simulation system using artificial neural networks for satellite data analysis and nonpoint source pollution models." [In Korean.] Ph.D. thesis, Dept. of Agricultural Engineering, Seoul National Univ.

Kang, M. S., and S. W. Park. 2003. "Development and application of total maximum daily loads simulation system using nonpoint source pollution model." *J. Korea Water Resour. Assoc.* 36 (1): 117–128. https://doi.org/10.3741/JKWRA.2003.36.1.117.

Kang, M. S., S. W. Park, J. J. Lee, and K. H. Yoo. 2006. "Applying SWAT for TMDL programs to a small watershed containing rice paddy fields." *Agric. Water Manage.* 79 (1): 72–92. https://doi.org/10.1016/j.agwat.2005.02.015.

Laniak, G. F., et al. 2013. "Integrated environmental modeling: A vision and roadmap for the future." *Environ. Model. Software* 39 (2013): 3–23. https://doi.org/10.1016/j.envsoft.2012.09.006.

Martin, P., E. LeBoeuf, J. Dobbins, E. Daniel, and M. Abkowitz. 2005. "Interfacing GIS with water resource models: A state-of-the-art review." *J. Am. Water Resour. Assoc.* 41 (6): 1471–1487. https://doi.org/10.1111/j.1752-1688.2005.tb03813.x.

Moore, R. V., and C. Tindall. 2005. "An overview of the open modelling interface and environment (the OpenMI)." *Environ. Sci. Policy* 8 (3): 279–286. https://doi.org/10.1016/j.envsci.2005.03.009.

Ning, S. K., K. Y. Cheng, N. B. Chang. 2002. "Evaluation of non-point sources pollution impacts by integrated 3S information technologies and GWLF model in the Kao-ping River Basin, Taiwan." *Water Sci. Technol.* 46 (6): 217–224.

Ramirez, C. M., J. H. Viers, J. F. Quinn, M. L. Johnson, B. Kozlowicz, and J. Florsheim. 2005. "Mass wasting identification in the Navarro River watershed using hyperspectral imagery." In *Proc., California and the World Ocean '02*, 1279–1288. Reston, VA: ASCE.

Richard, J. 1986. *Remote sensing digital image analysis: An introduction*, 281. New York: Springer.

Shafique, N., F. Fulk, and B. Autrey. 2003. "Hyperspectral remote sensing of water quality parameters for large rivers in the Ohio River basin." In *Proc., 1st Interagency Conf. on Research in the Watersheds*. Benson, AZ: USDA ARS Southwest Watershed Research Center at the Walnut Gulch Experimental Watershed.

Strager, M. P., J. J. Fletcher, J. M. Strager, C. B. Yuill, R. N. Eli, J. Todd Petty, and S. J. Lamont. 2010. "Watershed analysis with GIS: The watershed characterization and modeling system software application." *Comput. Geosci.* 36 (7): 970–976. https://doi.org/10.1016/j.cageo.2010.01.003.

USEPA. 2011. "Impaired waters and total maximum daily loads." Accessed July 15, 2017. http://water.epa.gov/lawsregs/lawsguidance/cwa/tmdl/.

Viers, J. H., C. M. Ramirez, J. F. Quinn, and M. L. Johnson. 2005. "The use of hyperspectral technologies to identify riparian habitats in coastal watersheds: An example from the Navarro River, California." In *Proc., California and the World Ocean '02*, 1377–1391. Reston, VA: ASCE.

Yuan, Y., R. L. Bingner, and J. Boydstun. 2006. "Development of TMDL watershed implementation plan using annualized AGNPS." *Land Use Water Resour. Res.* 6: 1–8.

Zaidi, A. 2012. "Water quality management using GIS and RS tools." In *Proc., World Environmental and Water Resources Congress 2012*, 842–848. Reston, VA: ASCE.

Zarco-Tejada, P., and V. González-Dugo. 2012. "Fluorescence, temperature and narrow-band indices acquired from a UAV platform for water stress detection using a micro-hyperspectral imager and a thermal." *Remote Sens. Environ.* 117: 322–337. https://doi.org/10.1016/j.rse.2011.10.007.

Zeiler, M. 1999. *Modeling our world. The ESRI guide to geodatabase design*. Redlands, CA: Environmental Systems Research Institute.